

PAPER

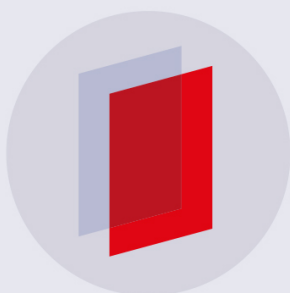
# Synthesis of magnetic Fe<sub>3</sub>O<sub>4</sub>/graphene oxide nanocomposites and their tribological properties under magnetic field

To cite this article: Arukali Sammaiah *et al* 2018 *Mater. Res. Express* **5** 105006

View the [article online](#) for updates and enhancements.

## Related content

- [One-step Preparation of graphene oxide/polypyrrole magnetic nanocomposite and its application in the removal of methylene blue dye from aqueous solution](#)  
Ali Afzali Nezhad, Mohammad Alimoradi and Majid Ramezani
- [Enhanced magnetic anisotropy and heating efficiency in multi-functional manganese ferrite/graphene oxide nanostructures](#)  
Anh-Tuan Le, Chu Duy Giang, Le Thi Tam et al.
- [Effect of modified graphene on thermal, mechanical and tribological performance of polyimide based composites](#)  
Duxin Li, Wenyan Yang, Yue Chen et al.



**IOP | ebooks™**

Bringing you innovative digital publishing with leading voices to create your essential collection of books in STEM research.

Start exploring the collection - download the first chapter of every title for free.

# Materials Research Express



## PAPER

# Synthesis of magnetic Fe<sub>3</sub>O<sub>4</sub>/graphene oxide nanocomposites and their tribological properties under magnetic field

RECEIVED  
18 May 2018

REVISED  
19 July 2018

ACCEPTED FOR PUBLICATION  
16 August 2018

PUBLISHED  
29 August 2018

Arukali Sammaiah, Wei Huang and Xiaolei Wang

College of Mechanical and Electrical Engineering, Nanjing University of Aeronautics & Astronautics, Nanjing 210016, People's Republic of China

E-mail: [huangwei@nuaa.edu.cn](mailto:huangwei@nuaa.edu.cn)

**Keywords:** Fe<sub>3</sub>O<sub>4</sub> nanoparticles, graphene oxide, magnetic field, friction, wear

Supplementary material for this article is available [online](#)

## Abstract

Nano and composite materials have received extensive research interest for improving tribological properties. In the present study, magnetic iron oxide/graphene oxide (Fe<sub>3</sub>O<sub>4</sub>/GO) nanocomposites were prepared by a simple and effective chemical co-precipitation method. The iron ions were generated and adsorbed onto the surface of GO in basic solution, followed by nucleation and growth of nanoparticles. The magnetic and structural properties of composites were investigated by vibrating sample magnetometer, Fourier transform infrared spectroscopy, x-ray powder diffraction, and transmission electron microscopy. Tribological properties of nanocomposites and pure Fe<sub>3</sub>O<sub>4</sub> nanoparticles were evaluated using a ball-plate tribotester. It was found that the nanoparticles and composites improved friction and wear performances with magnetic field. The test results reveal that an increase in the concentration of GO in nanocomposites, the friction coefficient decreased significantly, the maximum reduction by 35.5% compared with pure Fe<sub>3</sub>O<sub>4</sub> nanoparticles. The enhanced tribological performances of the nanocomposites can be explained by the combination of GO and magnetic nanoparticles.

## 1. Introduction

Magnetic fluids are kinetically stable colloidal suspensions of mono-domain magnetic nanoparticles dispersed in a liquid carrier and stabilized by means of suitable organic surfactant [1]. Previously these magnetic fluids were designed for sealing, ink-jet printing, damper, grinding, material separation and biomedicine due to its exceptional physical and chemical properties [2–5].

Currently, lubrication is becoming another important application for magnetic fluid. It can be confined, positioned, and controlled at desired locations as well as prevent from leaking and polluting the environment by applying external magnetic field [6–8]. Furthermore, the viscosity of magnetic fluid will be increased with the external magnetic field strength, which leads to the enhanced load carrying capacity in hydrodynamic regime [9]. Besides, many investigations on magnetic fluid lubrication becomes focusing on boundary lubrication. Tribological behavior of magnetic fluid was reported by Uhlman *et al.*, [10] and found that under boundary lubrication conditions, it can reduce the wear. The friction and wear properties on cylinder specimens constructed with permanent magnet of magnetic fluid were reported by Miyake and Takahashi [11]. They found that magnetic fluids decreased the friction and wear under low velocity condition in boundary lubricating regime.

Questions then rise: expect the carrier liquid of the magnetic fluid, what are the working mechanisms of magnetic particles while the surface becomes to contact in boundary lubrication regime? How about the effect of magnetic field? Can the traditional ferromagnetic particles be replaced in order to further improve the lubrication performance? There is still no available knowledge about this.

Among many magnetic particles (e.g.,  $\text{Fe}_3\text{O}_4$ , Ni-Fe, Co and  $\varepsilon\text{-Fe}_3\text{N}$ ),  $\text{Fe}_3\text{O}_4$  nanoparticles receives extensive research interest because of easy preparation [12, 13]. For  $\text{Fe}_3\text{O}_4$  nanoparticles, on one hand, the nearly spherical particles usually supposed to have good lubricating effect by rolling friction mechanism [14]. On the other hand, because of high surface energies and heavy aggregation of particles it may be shows higher friction values, particularly in magnetic field. Hence, to figure out this issue, friction tests lubricated with pure  $\text{Fe}_3\text{O}_4$  nanoparticles were carried out. Beside, to further improve the lubrication property of  $\text{Fe}_3\text{O}_4$  nanoparticles, composite materials  $\text{Fe}_3\text{O}_4$ /graphene oxide (GO) was designed. Due to graphene has a traditional solid lubricant material for reducing adhesion, friction and wears [15–17]. Comparing with graphene, GO having polar oxygenated functional groups, such as epoxides, carbonyl, carboxyl and hydroxyl groups. These functional groups can serve as nucleation sites for metal ions to constructing graphene based composite materials. Various methods were reported for preparation of  $\text{Fe}_3\text{O}_4$ /GO *in situ* formation [18], hydrothermal method [19], solvothermal method [20], chemical precipitation [21] and covalent bonding method [22].  $\text{Fe}_3\text{O}_4$ /GO nanocomposites have been demonstrated for wide range of applications such as lithium ion batteries [23], dye removal [24], drug delivery [25], and used in nanocomposite formulation as a magnetic component [26]. However, there has been no literature so far investigating the magnetically functionalized  $\text{Fe}_3\text{O}_4$ /GO composites in the application of friction under magnetic field.

In this work, we have proposed to developing nanocomposites containing iron oxide and graphene oxide for lubrication. The nanocomposites were synthesized via co-precipitation method on GO with different weight ratios of  $\text{Fe}_3\text{O}_4$ . The resultant composites were fully characterized for understand their structure and functionalities. Finally, the tribological properties of the nanocomposites were evaluated with and without magnetic field. In addition, the lubricating mechanism of magnetic  $\text{Fe}_3\text{O}_4$ /GO nanocomposites is discussed.

## 2. Experimental

### 2.1. Materials

Graphene powder was purchased from XFNANO Advanced Materials Supplier, Nanjing, China. Ferric chloride ( $\text{FeCl}_3 \cdot 6\text{H}_2\text{O}$ ) and ferrous chloride ( $\text{FeCl}_2 \cdot 4\text{H}_2\text{O}$ ) were supplied by Xilong Scientific Co., Ltd (Guangdong, China). Sodium nitrate, sulfuric acid ( $\text{H}_2\text{SO}_4$ ), potassium permanganate ( $\text{KMnO}_4$ ), hydrochloric acid (HCl), sodium hydroxide (NaOH), ethylene glycol and aqueous hydrogen peroxide (30%) were purchased from KeLong Chemicals Co., Ltd (Chengdu, China). All of the chemicals were of analytical grade and used directly without purification.

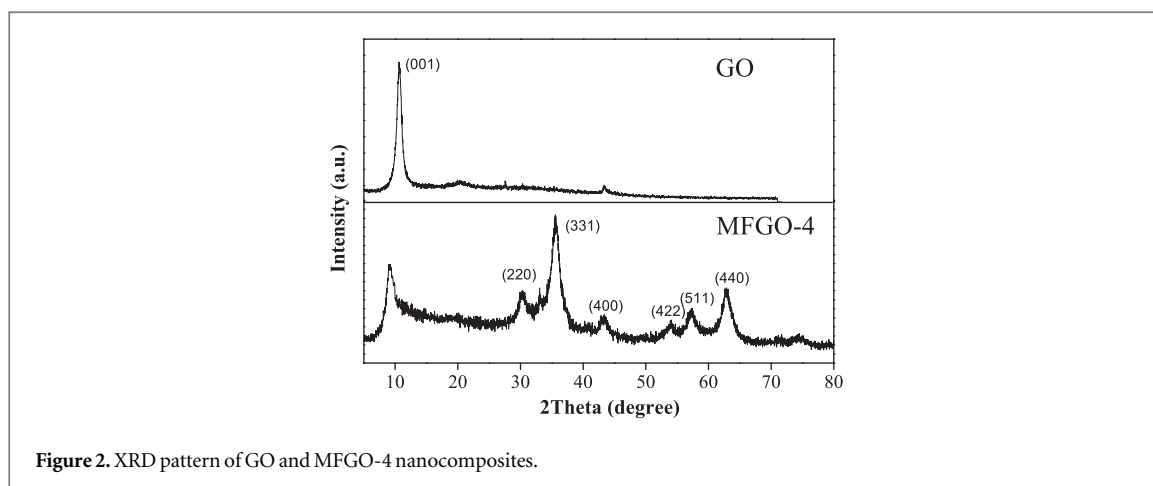
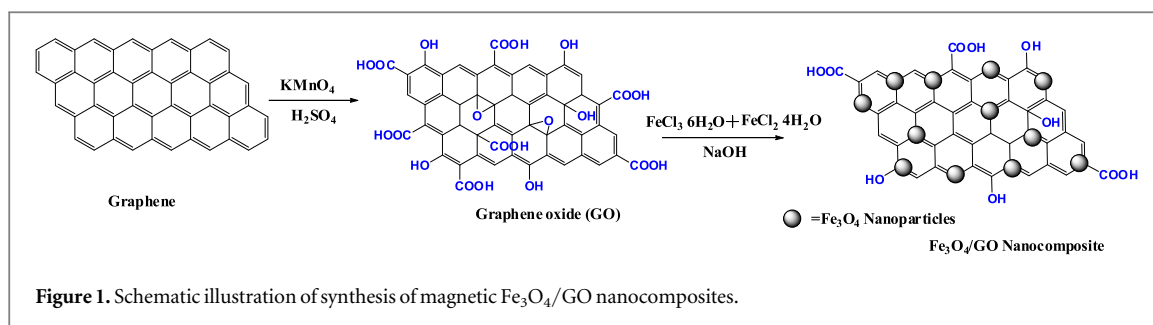
### 2.2. Synthesis of magnetic $\text{Fe}_3\text{O}_4$ /graphene oxide (MFGO) nanocomposites

Graphene oxide was prepared according to reported Hummers method with slight modifications [27] and MFGO nanocomposites were prepared by chemical precipitation method. Briefly, ferrous chloride and ferric chloride were dissolved in distilled water (100 ml) in a 1:2 molar ratio with an initial pH of less than 2. Then NaOH (1 M) was added drop wise into the above mixture to adjusted pH 4 because at low pH GO sheets are stack together [28]. Subsequently, GO (0.2 g in 100 ml deionized) suspension was prepared under ultrasonication. GO suspension was added slowly into the above mixture and then reaction further continued at room temperature for 30 min to form a homogeneous and stable mixture. To this solution of NaOH was added in a drop wise manner until pH 10 and the reaction mixture was stirred another 1 h while monitoring the reaction the color was changed from light brown to black. The product was collected by centrifugation and washed with deionized water several times until the pH of the supernatant was neutral and final product was dried an oven for 24 h at  $60^\circ\text{C}$ . The MFGO composites with different  $\text{Fe}_3\text{O}_4$  content were synthesized by changing the weight ration of  $\text{Fe}^{+3}$  to GO ( $\text{mFe}^{+3}:\text{mGO} = 1:1, 2:1, 4:1$  and  $8:1$ ) to obtained four samples of MFGO composites (MFGO-1, MFGO-2, MFGO-3 and MFGO-4 respectively). The pure magnetic  $\text{Fe}_3\text{O}_4$  nanoparticles was also prepared in similar procedure without addition of GO.

For evaluating the tribological properties, the MFGO composites and  $\text{Fe}_3\text{O}_4$  nanoparticles were dispersed in ethylene glycol; the weight concentration of sample was  $5 \text{ mg ml}^{-1}$  and ultrasonication for 30 min. Solid film formed on the surface of the stainless steel plate using a spin-coater with 2 ml of above mixture and ethylene glycol evaporated in oven.

### 2.3. Characterization

XRD analysis of the products were recorded with an X'Pert PRO x-ray diffract meter with  $\text{Co K}\alpha$  radiation ( $\lambda = 1.7886 \text{ \AA}$ ) with ranging from  $5^\circ$  to  $80^\circ$  at a scanning rate of  $2^\circ/\text{min}$  (scan step  $0.02^\circ$ ). The morphology of the nanocomposites was analyzed by transmission electron microscopy using a JEM-200CX (JEOL) at an accelerating voltage of 200 kV. The functional groups of nanocomposites were analyzed by Fourier transform infrared spectroscopy (FTIR) on NEXUS870 spectrometer (NICOLET) using KBr pellets in the range of



400–4000 cm<sup>-1</sup>. Magnetic susceptibility was measured using a vibrating sample magnetometer LDJ9600 in the magnetic field sweeps of –20 000 Oe to 20 000 Oe at room temperature.

#### 2.4. Tribological test

The tribological performance of the nanocomposites was conducted on a reciprocating sliding tribometer (Sinto Scientific, Japan). It consists of stationary holder with bearing ball of 10 mm in diameter and reciprocating table with a commercial 304 stainless steel plate, which both are non-magnetic. The permanent magnet was placed under the steel plate and length of magnet 10 mm, which was perpendicular to the reciprocating motion. The tests were conducted with sliding frequency of 0.83 Hz and stroke of 10 mm (average speed of 50 mm s<sup>-1</sup>). The friction time and load were 1500 s and 5 N, respectively. After the test, stainless steel plates were cleaned in deionized water by using ultrasonic bath for 15 min. The roughness of the stainless steel plate, as well as the 3D-topography of wear scars analyzed. The chemical composition on the worn surfaces was analyzed by the scanning electron microscopy (SEM) coupled with energy dispersive x-ray spectrometer (EDS).

### 3. Results and discussion

The composites were prepared by the precipitation of Fe<sub>3</sub>O<sub>4</sub> onto graphene oxide sheets as shown in figure 1. Initially graphite was reacted with H<sub>2</sub>SO<sub>4</sub> and KMnO<sub>4</sub> to obtained GO, which having a variety of polar oxygenated functional groups like carboxylic acid (–COOH), Hydroxy (–OH), and epoxy (–COC–). Then iron salts to form [Fe(H<sub>2</sub>O)<sub>6</sub>]<sup>3+</sup> and [Fe(H<sub>2</sub>O)<sub>6</sub>]<sup>2+</sup> iron aqua complexes with water. These complexes are coordinated with oxygen containing moieties on the surface of GO and then with the addition of NaOH, those complexes goes to hydrolysis to obtained MFGO composites. During the preparation of MFGO nanocomposites, GO undergo partial reduction due to the partial removal of epoxide and carboxylic acids under alkaline medium. Fe<sub>3</sub>O<sub>4</sub> nano particles are formed large aggregates due to dipolar interactions, which were efficiently prevented by GO through steric hindrance [23]. The products have been characterized adequately with various techniques shown below.

Figure 2 showed the XRD patterns of GO and MFGO-4 nanocomposites. The characteristic sharp diffraction peak at 10.5° was corresponding to the crystal plane (001) of GO [29]. For MFGO-4 composites, the characteristic peaks belonging to the Fe<sub>3</sub>O<sub>4</sub> and GO could be identified. The characteristic peaks at 2θ = 30.26, 35.52, 43.46, 54.5, 57.32, and 63.24° were attributed to the (220), (331), (400), (422), (511), and (440) planes of Fe<sub>3</sub>O<sub>4</sub> respectively (JCPDS 19-629), which indicating the formation of cubic spinel structure of the magnetic

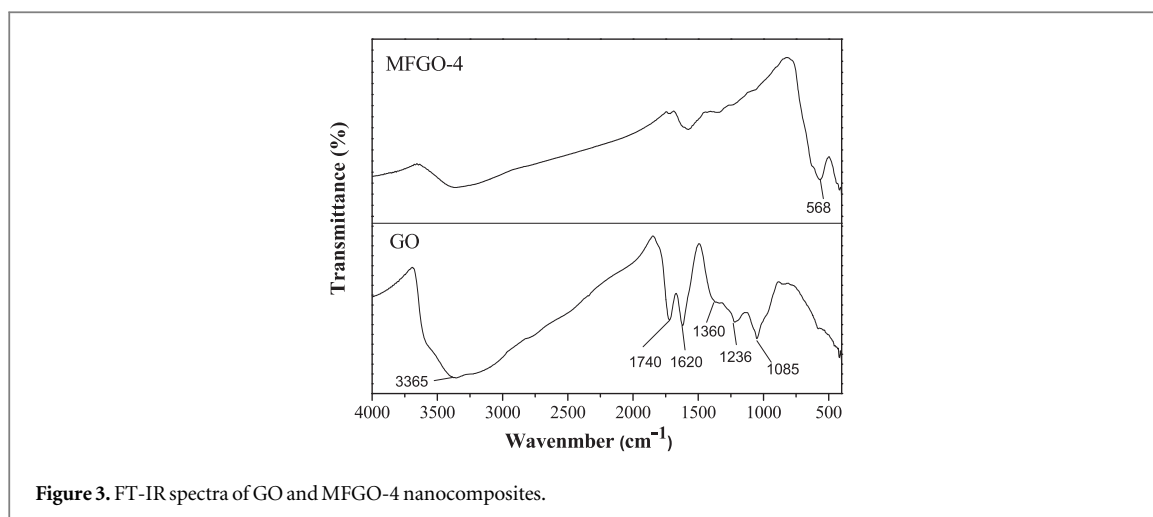


Figure 3. FT-IR spectra of GO and MFGO-4 nanocomposites.

materials. These peaks intensity were decreased in case of MFGO-3, MFGO-2 and MFGO-1 due to its low concentration of  $\text{Fe}_3\text{O}_4$  nanoparticles (see figure S1 is available online at [stacks.iop.org/MRX/5/105006/mmedia](https://stacks.iop.org/MRX/5/105006/mmedia)). The diffraction peak of GO was shifted toward a lower at  $2\theta = 9.2^\circ$  due to the partial reduction of GO. The results confirmed that MFGO nanocomposites having a mixture of two different phases such as cubic phase of  $\text{Fe}_3\text{O}_4$  and GO.

FT-IR spectra of GO and MFGO nanocomposites are shown figures 3 and S2. In spectrum of GO showed a strong absorption peak at  $1236\text{ cm}^{-1}$  and  $3365\text{ cm}^{-1}$  due to the bending and stretching vibrations of the  $-\text{OH}$ , respectively. The  $\text{C}=\text{O}$  stretching of carboxylic acid was observed at  $1740\text{ cm}^{-1}$ . The absorption peak at  $1360\text{ cm}^{-1}$  is corresponding to the bending vibration carboxyl group ( $\text{O}-\text{C}=\text{O}$ ) and absorption peak at  $1085\text{ cm}^{-1}$  could be alkoxy ( $\text{C}-\text{O}$ ) stretching vibration. Absorption peak at  $1620\text{ cm}^{-1}$  was observed due to the unoxidized aromatic  $\text{C}=\text{C}$  skeletal vibrations [30]. The IR spectrum of MFGO-4 composite differs from initial GO as indicated by the weakening of the carboxyl and hydroxy groups at  $1740$  and  $3365\text{ cm}^{-1}$ , respectively. More importantly, the vibration band at  $568\text{ cm}^{-1}$  was observed, corresponding to the  $\text{Fe}-\text{O}$ , which indicated that the  $\text{Fe}_3\text{O}_4$  nanoparticles were grafted on the GO sheet [31].

The morphology of the products was investigated by TEM. Figures 4(a)–(b) shows that pure GO has a crumpled and rippled structure and also it's clearly transparent. Figures 4(c)–(d) presents the spherical morphology and narrow size distribution of  $\text{Fe}_3\text{O}_4$  nano particles. It is clearly shown in figures 4(e)–(f) of the MFGO-4 composites, compared to the pure GO (figures 4(a)–(b)). It can be observed that  $\text{Fe}_3\text{O}_4$  particles are well distributed on the GO surface. It is also observed, there is no large area of the GO sheets without  $\text{Fe}_3\text{O}_4$  decoration and isolated  $\text{Fe}_3\text{O}_4$  nano particles were absent beyond the GO. Moreover, aggregations of nano particles are not observed on the GO sheet, suggesting a strong interaction between the GO sheets and magnetic nanoparticles. The selected area electron diffraction (SAED) pattern is shown in inserted figures 4(b) and (f) of the GO and MFGO-4 nanocomposites. The bright diffraction rings indicate its highly crystalline nature of GO. The SAED pattern of MFGO-4 reveals that sample having a mixture of two different phases such as highly crystalline and cubic structure, which are similar to the standard diffraction pattern of pure GO and  $\text{Fe}_3\text{O}_4$  (figures 4(d)) [19].

The magnetic properties of  $\text{Fe}_3\text{O}_4$  nanoparticles and MFGO composites were characterized by using VSM at room temperature. Figure 5 shows the magnetization hysteresis loops of all samples with an applied magnetic field sweeping from  $-20\,000$  to  $20\,000$  Oe. They are S-like curves with small coercivities, indicating that all the nano composites are ferromagnetic behavior. The saturation magnetization for  $\text{Fe}_3\text{O}_4$ , MFGO-4, MFGO-3, MFGO-2 and MFGO-1 were  $28.1$ ,  $12.4$ ,  $8.4$ ,  $3.8$  and  $1.3\text{ emu} \cdot \text{g}^{-1}$ , respectively. The saturation magnetization values of the nanocomposites are much smaller than that of pure  $\text{Fe}_3\text{O}_4$  and the values decrease with the increment of GO loading amount. This could be due to the existence of the magnetically inactive GO, and this effect become more pronounced as partial size decreases [22].

The friction and wear properties of the  $\text{Fe}_3\text{O}_4$  nanoparticles and nanocomposites were evaluated in the presence and absence of a magnetic field. Figure 6(a) shows the friction coefficients of  $\text{Fe}_3\text{O}_4$  nanoparticles with different magnetic field ( $H$ ) of  $0$ ,  $50$  and  $100\text{ mT}$ . As can be seen in figure 6(a), the friction coefficient of nanoparticles was reduced significantly with increasing the magnetic field.  $\text{Fe}_3\text{O}_4$  nanoparticles are randomly oriented in the case of without magnetic field. During the friction process, these particles can be squeezed out the contact area and directly contact between the tribo-pairs happens. As is known, each particle can be considered as a thermally agitated permanent magnet. In the presence external magnetic field, magnetic particles are aligned to the applied magnetic field direction (see figure 6(a) inset). Meanwhile, the magnetic forces of individual

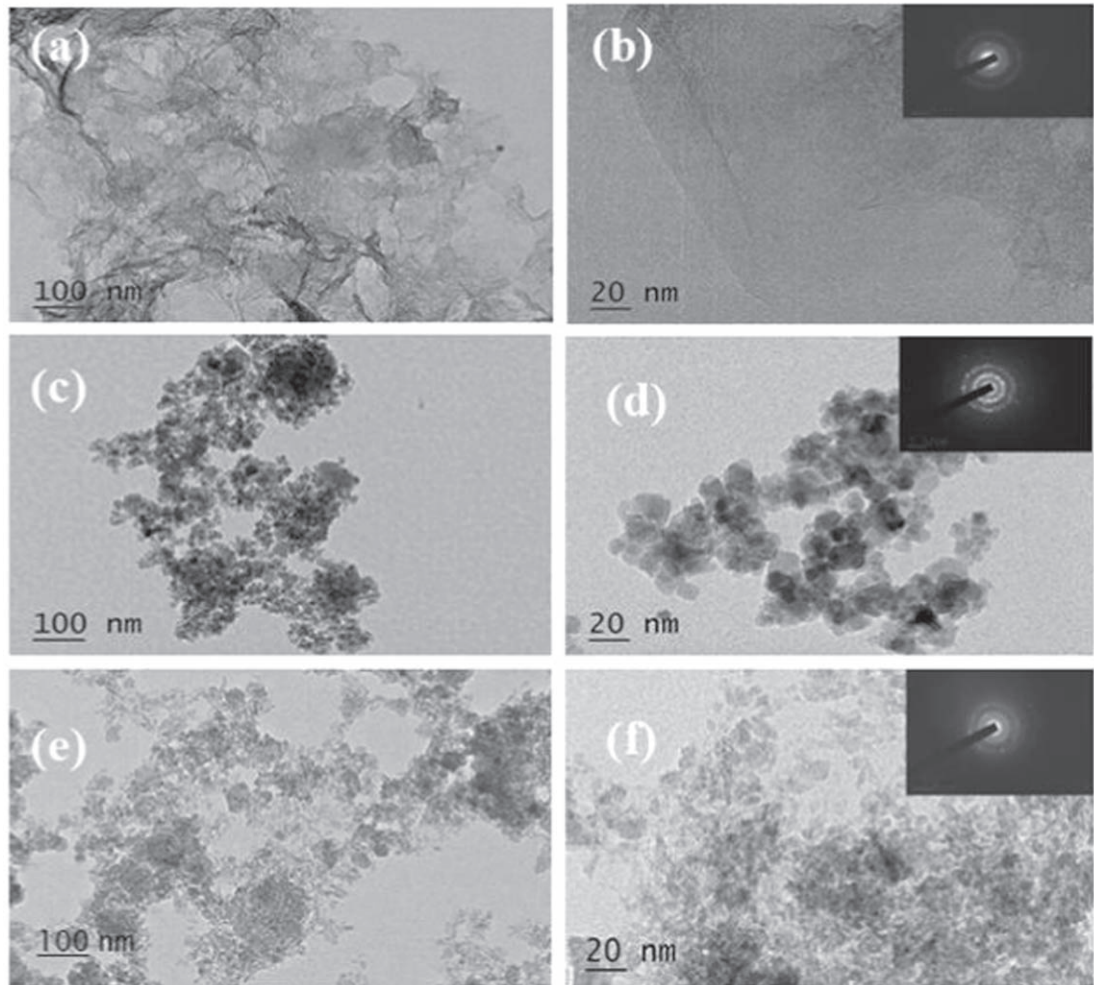


Figure 4. TEM images of (a)–(b) GO, (c)–(d)  $\text{Fe}_3\text{O}_4$  and (e)–(f) MFGO-4 nanocomposites.

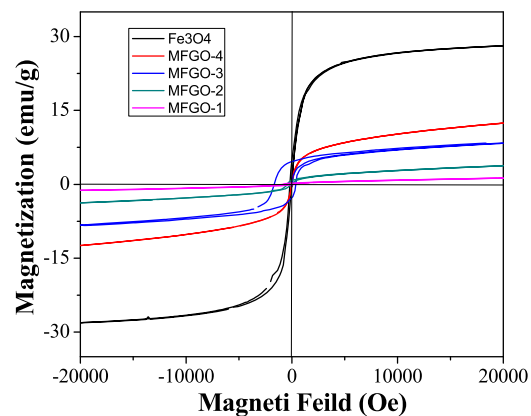
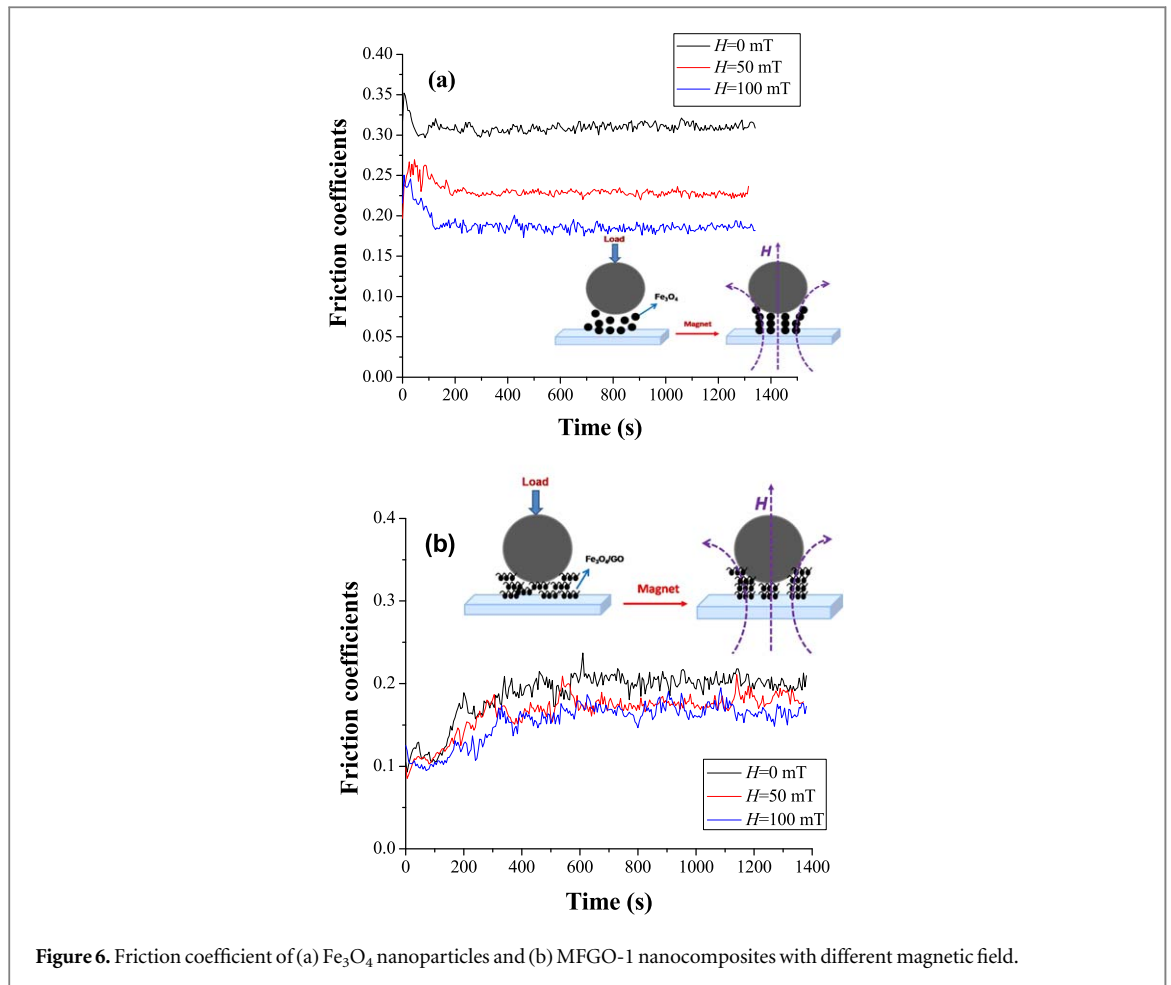


Figure 5. Magnetization curves of  $\text{Fe}_3\text{O}_4$  nanoparticles and MFGO nanocomposites.

particles due to magnetization may act as supporting force, exhibiting load carrying capacity. The higher of the external magnetic field it is, the greater of the aforementioned force. Thus, the friction force may only come from the shear of the magnetized particles, and it decreases with the increasing of magnetic field.

Figure 6(b) gives the coefficients of MFGO-1 nanocomposites. The friction coefficients increase at the beginning of the test. At the beginning of the test, lots of MFGO particles are in the contact zone. Therefore, low friction coefficients appear. As the test going on, parts of MFGO particles are squeezed out the contact area, thus friction coefficient increases gradually. After a period of the time, the coefficients maintain stable. The observed



**Figure 6.** Friction coefficient of (a) Fe<sub>3</sub>O<sub>4</sub> nanoparticles and (b) MFGO-1 nanocomposites with different magnetic field.

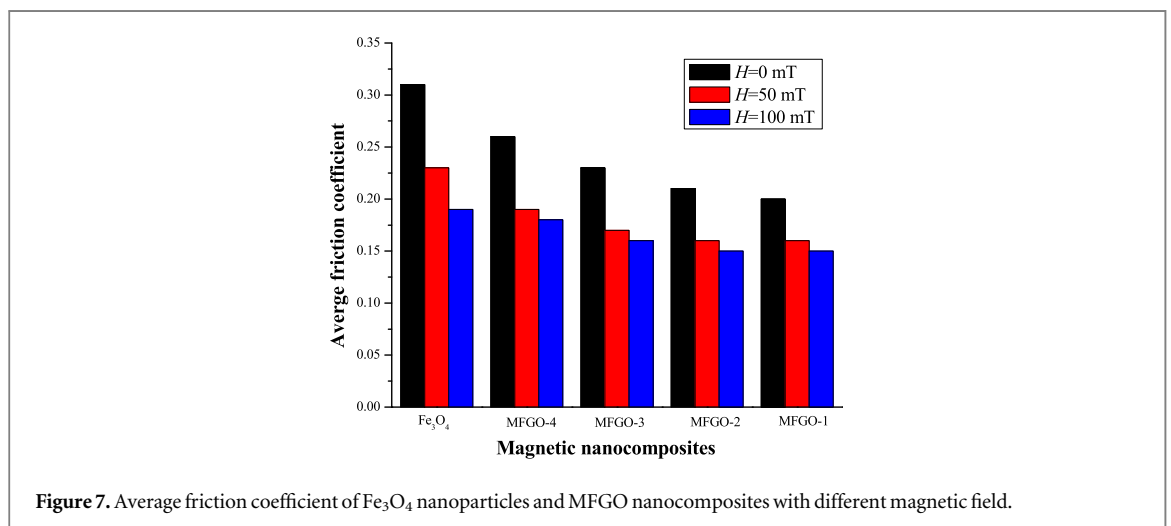


**Figure 7.** Average friction coefficient of Fe<sub>3</sub>O<sub>4</sub> nanoparticles and MFGO nanocomposites with different magnetic field.

trend of the friction coefficient of nanocomposites is similar to that of Fe<sub>3</sub>O<sub>4</sub>. But nanocomposites having low friction coefficient values than pure nanoparticles due to presence of GO. However, the decreasing trend of the friction coefficient in composites is less than that of pure Fe<sub>3</sub>O<sub>4</sub>. This is due to the low content of Fe<sub>3</sub>O<sub>4</sub> in the nanocomposites, corresponding to the lower magnetization compared to the pure nanoparticles (see in figure 5).

Figure 7 shows the average friction coefficient of pure Fe<sub>3</sub>O<sub>4</sub> nanoparticles and MFGO composites. The effect of magnetic field is obvious. It can be observed that the average friction coefficient decreases with increasing the magnetic field. Whenever there is magnetic field, friction coefficients of Fe<sub>3</sub>O<sub>4</sub> is higher than that of the MFGO nanocomposites. As expected, GO sheets with large area size could be exposed and act as self lubricated carbon film on the rubbing surface [32]. The uniform and self lubricating thin carbon film reduces

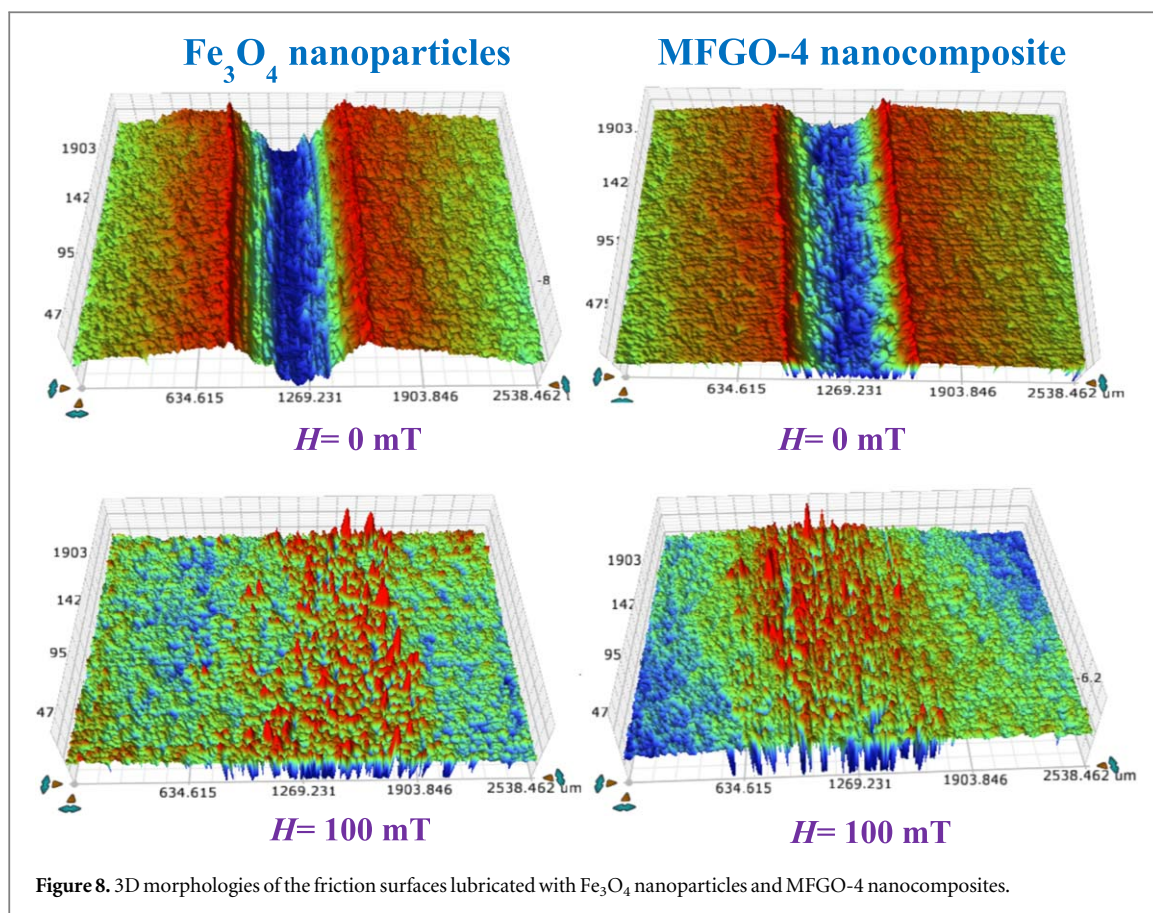


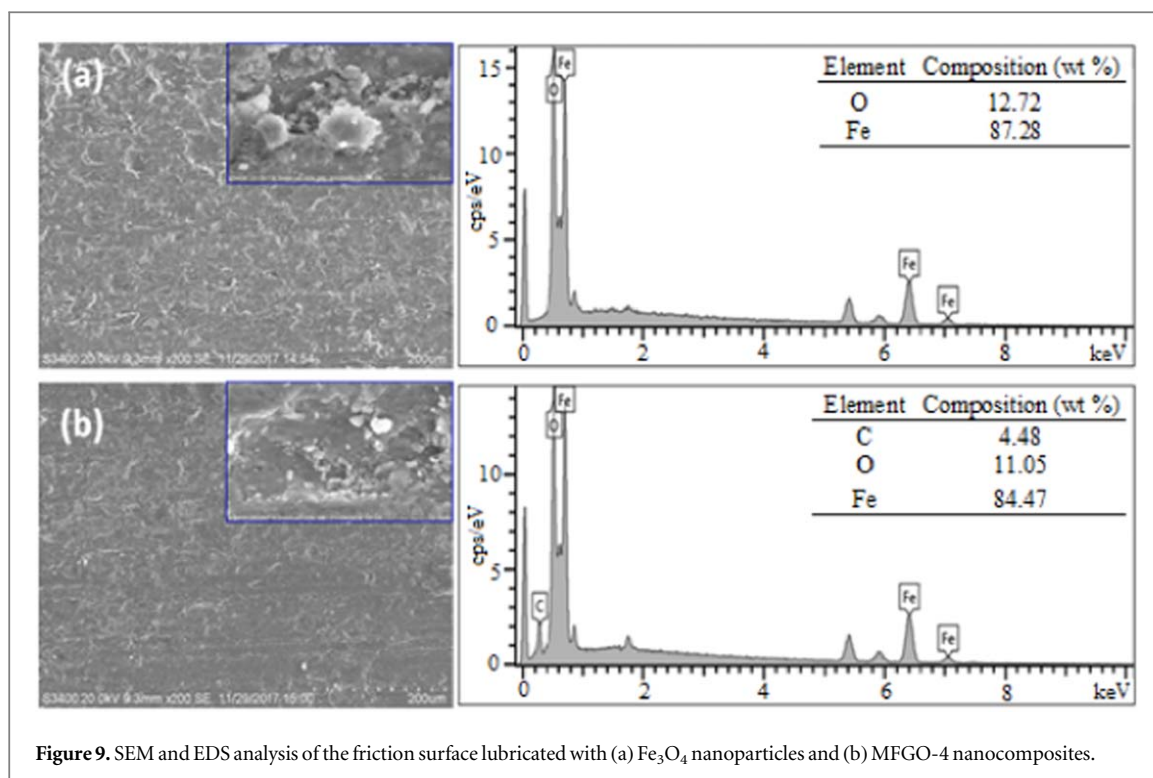
Figure 8. 3D morphologies of the friction surfaces lubricated with  $\text{Fe}_3\text{O}_4$  nanoparticles and MFGO-4 nanocomposites.

friction between the composite and the steel counterpart. The friction coefficient of MFGO composites decreased with increasing the GO concentration. Among the all nanocomposites, MFGO-1 with high content of GO exhibits lower friction coefficient value, with maximum reduction by 35.5%.

For better understanding the tribological mechanism of the  $\text{Fe}_3\text{O}_4$  nanoparticles and MFGO nanocomposites, the worn surface of the stainless steel plate lubricated by magnetic compounds with different magnetic field were observed. Figure 8 shows 3D profiles of wear tracks of stainless steel plates, lubricated with  $\text{Fe}_3\text{O}_4$  and MFGO-4 films, respectively. As shown in figure 8, wear scar depths were reduced under the magnetic field ( $H = 100$  mT). The  $\text{Fe}_3\text{O}_4$  corresponding wear depths on friction surface are 11.7, and 1.5  $\mu\text{m}$  with 0 and 100 mT magnetic fields respectively. The wear depths on the friction surface are 11.5, and 1.2  $\mu\text{m}$  with 0 and 100 mT magnetic field respectively, which are corresponding to the MFGO-4 nanocomposites. Whenever there is no magnetic field, nanoparticles exhibits high depths due to the nanoparticles can be squeezed out from contact zone under sliding condition. In the presence of external magnetic field, the most of the magnetic particles are retained within the contact zone, thus decreases the wear depth. The similar results were observed for nanocomposites.

Figure 9 shows the SEM and EDS of the friction surfaces lubricated with the (a)  $\text{Fe}_3\text{O}_4$  nanoparticles and (b) MFGO-4 nanocomposites. Compared with  $\text{Fe}_3\text{O}_4$  particles, the friction surface lubricated with nanocomposites is slightly smothered, and wear damage is minimal. Clearly, the magnetic nanocomposites could produce a low shear stress sliding on the worn surface due to formation of the surface protective lubricating carbon film. EDX analysis shows the presence of carbon on the friction surface lubricated with nanocomposites whereas carbon element was absent in the EDX of  $\text{Fe}_3\text{O}_4$  nanoparticles. Both the self lubricating carbon thin film effects of GO and rolling effects of  $\text{Fe}_3\text{O}_4$  nanoparticles makes nanocomposites exhibited lower friction and wear.

According to the above analysis, we are proposing the possible mechanism behind reducing friction of nanocomposites. Magnetic  $\text{Fe}_3\text{O}_4$ /GO nanocomposites have excellent tribological properties. Under the sliding conditions, GO nano sheets with large surface area could be exposed and exist stably on the rubbing surface. With the formation of self lubricating thin carbon film of GO and rolling effect of  $\text{Fe}_3\text{O}_4$  nanoparticles reduces friction and wear of MFGO nanocomposites. The friction behavior of the magnetic materials can be strongly influenced by the presence of a magnetic field. In the interface of magnetized sliding contact, most of the magnetic particles are attracted to each other due to magnetic force, and a particle bridge is formed on the surface of the substrate, which can provide the extra supporting force to tribo-pair. Thus, decrease the friction coefficient with the magnetic field.



#### 4. Conclusions

In this work, the tribological properties of Fe<sub>3</sub>O<sub>4</sub> nanoparticles and magnetic Fe<sub>3</sub>O<sub>4</sub>/GO nanocomposites were investigated under magnetic field. The magnetic nanoparticles fabricated on GO sheets were synthesized using co-precipitation method and characterized. The results show that Fe<sub>3</sub>O<sub>4</sub> nanoparticles have been successfully decorated on the surface of GO. Increasing the weight ratio of Fe<sup>+3</sup> to GO increases the magnetic strength of the nanocomposites. The Fe<sub>3</sub>O<sub>4</sub>/GO nanocomposites exhibit excellent tribological properties. All the Fe<sub>3</sub>O<sub>4</sub>/GO nanocomposites improved the tribological properties and exhibited better performance compared to pure Fe<sub>3</sub>O<sub>4</sub> nanoparticles. Under the magnetic field, both pure Fe<sub>3</sub>O<sub>4</sub> nanoparticles and Fe<sub>3</sub>O<sub>4</sub>/GO nanocomposites shows better friction and wear properties than without magnetic field. In addition, the synthesized products can be further extending to create a wide range of various functional nanocomposites.

#### Acknowledgments

The authors are grateful for the support provided by the Fundamental Research Funds for the Central Universities (No. NE2017104).

#### ORCID iDs

Wei Huang <https://orcid.org/0000-0002-8871-634X>

Xiaolei Wang <https://orcid.org/0000-0002-9055-1011>

#### References

- [1] Fannin P C 2004 Characterisation of magnetic fluids *J. Alloy. Compd.* **369** 43–51
- [2] Kanno T, Kouda Y, Takeishi Y, Minagawa T and Yamamoto Y 1997 Preparation of magnetic fluid having active-gas resistance and ultra-low vapor pressure for magnetic fluid vacuum seals *Tribol. Int.* **30** 701–5
- [3] Nakatsuka K 1993 Trends of magnetic fluid applications in Japan *J. Magn. Magn. Mater.* **122** 387–94
- [4] Umehara N and Komanduri R 1996 Magnetic fluid grinding of HIP-Si<sub>3</sub>N<sub>4</sub> rollers *Wear* **192** 85–93
- [5] Rheinländer T, Kötz R, Weitschies W and Semmler W 2000 Magnetic fluids: biomedical applications and magnetic fractionation *Magn. Electr. Sep.* **10** 179–99
- [6] Huang W and Wang X 2008 Preparation and properties of ε-Fe<sub>3</sub>N-based magnetic fluid *Nanoscale Res. Lett.* **3** 260–4
- [7] Shen C, Huang W, Ma G L and Wang X 2009 A novel surface texture for magnetic fluid lubrication *Surf. Coat. Technol.* **204** 433–9
- [8] Deysarkar A K and Clampitt B H 1988 Evaluation of ferrofluids as lubricants *J. Synth. Lubr.* **5** 105–14
- [9] Odenbach S 2003 Ferrofluids-magnetically controlled suspensions *Colloids Surfaces A: Physicochem. Eng. Asp.* **217** 171–8

- [10] Uhlmann E, Spur G, Bayat N and Patzwald R 2002 Application of magnetic fluids in tribotechnical systems *J. Magn. Magn. Mater.* **252** 336–40
- [11] Miyake S and Takahashi S 1985 Sliding bearing lubrication with ferromagnetic fluid *Tribol. Trans.* **28** 461–6
- [12] Huang W and Wang X 2016 Ferrofluids lubrication: a status report *Lubri. Sci.* **28** 3–26
- [13] Huang W, Wang X, Ma G and Shen C 2009 Study on the synthesis and tribological property of Fe<sub>3</sub>O<sub>4</sub> base magnetic fluids *Tribol. Lett.* **33** 187–92
- [14] Huang W, Shen C, Liao S and Wang X 2011 Study on the ferrofluid lubrication with an external magnetic field *Tribol. Lett.* **41** 145–51
- [15] Berman D, Erdemir A and Sumant A V 2014 Graphene: a new emerging lubricant *Mater. Today* **17** 31–42
- [16] Liang S, Shen Z, Yi M, Liu L, Zhang X and Ma S 2016 *In situ* exfoliated graphene for high-performance water-based lubricants *Carbon* **96** 1181–90
- [17] Kim K S, Lee H J, Lee C, Lee S K, Jang H and Ahn J H 2011 Chemical vapor deposition-grown graphene: the thinnest solid lubricant *ACS Nano* **5** 5107–14
- [18] Singh V K, Patra M K, Manoth M, Gowd G S, Vadera S R and Kumar N 2009 *In situ* synthesis of graphene oxide and its composites with iron oxide *New Carbon Mater.* **24** 147–52
- [19] Wu H, Gao G, Zhou X, Zhang Y and Guo S 2012 Control on the formation of Fe<sub>3</sub>O<sub>4</sub> nanoparticles on chemically reduced graphene oxide surfaces *Cryst. Eng. Comm.* **14** 499–504
- [20] Zhan Y, Meng F, Lei Y, Zhao R, Zhong J and Liu X 2011 One-pot solvothermal synthesis of sandwich-like graphene nano sheets/Fe<sub>3</sub>O<sub>4</sub> hybrid material and its micro wave electromagnetic properties *Mater. Lett.* **65** 1737–40
- [21] Chandra V, Park J, Chun Y, Lee J W, Hwang I and Kim K S 2010 Water-dispersible magnetite-reduced graphene oxide composites for arsenic removal *ACS Nano* **4** 3979–86
- [22] He F, Fan J, Ma D, Zhang L, Leung C and Chan H L 2010 The attachment of Fe<sub>3</sub>O<sub>4</sub> nanoparticles to graphene oxide by covalent bonding *Carbon* **48** 3139–44
- [23] Su J, Cao M, Ren L and Hu C 2011 Fe<sub>3</sub>O<sub>4</sub>-graphene nanocomposites with improved lithium storage and magnetism properties *J. Phys. Chem. C* **115** 14469–77
- [24] Xie G, Xi P, Liu H, Chen F, Huang L, Shi Y, Hou F, Zeng Z, Shao C and Wang J 2012 A facile chemical method to produce superparamagnetic graphene oxide-Fe<sub>3</sub>O<sub>4</sub> hybrid composite and its application in the removal of dyes from aqueous solution *J. Mater. Chem.* **22** 1033–9
- [25] Yang X, Zhang X, Ma Y, Huang Y, Wang Y and Chen Y 2009 Superparamagnetic graphene oxide-Fe<sub>3</sub>O<sub>4</sub> nanoparticles hybrid for controlled targeted drug carriers *J. Mater. Chem.* **19** 2710–24
- [26] Kassaei M Z, Motamedi E and Majidi M 2011 Magnetic Fe<sub>3</sub>O<sub>4</sub>-graphene oxide/polystyrene: fabrication and characterization of a promising nanocomposites *Chem. Eng. J.* **172** 540–9
- [27] Hummers W S and Offeman R E 1958 Preparation of graphitic oxide *J. Am. Chem. Soc.* **80** 1339
- [28] Zubir N A, Zhang X, Yacou C and Diniz da Costa J C 2014 Fenton-like degradation of acid orange 7 using graphene oxide-iron oxide nanocomposites *Sci. Adv. Mater.* **6** 1–7
- [29] Xu J, Wang K, Zu S, Han B and Wei Z 2010 Hierarchical nanocomposites of polyaniline nano wire arrays on graphene oxide sheets with synergistic effect for energy storage *ACS Nano* **4** 5019–26
- [30] Stankovich S, Piner R D, Nguyen S T and Ruoff R S 2006 Synthesis and exfoliation of isocyanate-treated graphene oxide nano platelets *Carbon* **44** 3342–7
- [31] Bai L Z, Zhao D L, Xu Y, Zhang J M, Gao Y L and Zhao L Y 2012 Inductive heating property of graphene oxide-Fe<sub>3</sub>O<sub>4</sub> nanoparticles hybrid in an AC magnetic field for localized hyperthermia *Mater. Lett.* **68** 399–401
- [32] Liang H, Bu Y, Zhang J, Cao Z and Liang A 2013 Graphene oxide film as solid lubricant *ACS Appl. Mater. Interfaces* **5** 6369–75